

Properties of silver-tin alloys obtained from pyrophosphate-cyanide electrolytes containing EDTA salts

Antoaneta Hrussanova · I. Krastev ·
G. Beck · A. Zielonka

Received: 29 January 2010 / Accepted: 5 September 2010 / Published online: 26 September 2010
© Springer Science+Business Media B.V. 2010

Abstract Silver-tin alloy coatings are electrodeposited from a newly developed EDTA containing cyanide-pyrophosphate electrolyte and some properties of the obtained coatings, such as microhardness, internal stress, abrasion resistance, plug-in forces and electrical contact resistance depending upon the applied current density or the tin content of the alloy, respectively, are investigated. The co-deposition of tin leads to the change of the tensile stress of pure silver coatings to compressive stress in the formed solid solution of the alloy and to almost stress free coatings at high current densities. The microhardness runs over a maximum at current densities, where the silver lattice is saturated with tin and the deposition of phase heterogeneous coatings starts. The abrasion resistance diminishes at increased tin content, and the changes of the electrical contact resistance are in the opposite direction. The measured plug-in forces show the lubricating properties of the alloy coatings.

Keywords Silver-tin alloys · Electrodeposition · Electrolytes · Spatio-temporal structures

1 Introduction

Silver alloys with tin are important because of their improved corrosion and tarnish resistance (at high silver contents in the alloy) compared to pure silver, as well as for their better physico-mechanical properties and increased melting point (at high tin contents) compared to pure tin, the latter being important when several contact elements for the electronics are plated. The physical properties of Ag-Sn alloys are established in detail a long time ago [1]. The best and relatively long-lasting strength properties are observed in the eutectic alloy [2]. Alloys with 2.5–5 wt% Ag show higher resistance to plastic deformations compared to pure tin [2], and alloys with 11 wt% Ag form solder joints with 2–4 times higher strength properties than pure tin or tin–lead alloys [3].

Investigations on the properties of silver-tin coatings from pyrophosphate or pyrophosphate-cyanide electrolytes show, that alloys with about 5–7 or 10 wt% Sn have a significantly better tarnish resistance compared to pure silver [4, 5]. Alloys with 10 wt% Sn exhibit good ductility and solderability and have a low friction coefficient [5]. The resistivity of this Ag-Sn alloy (10 wt% Sn) is 30 $\mu\Omega$ cm. This value is higher than that of unalloyed silver (1.66–1.85 $\mu\Omega$ cm) but it is representative as a typical value for the resistivity of an alloy [5]. A number of authors have studied the microhardness of silver-tin alloys [6–9]. The increase in tin content leads to a decrease in the microhardness of the alloy [6, 8, 9]. Grekova and Vyacheslavov [7] show that the highest values in the curves for microhardness, the specific electrical resistivity and the contact resistance are obtained at tin contents corresponding to the α -, ζ - and ε -phases (5, 15, 28 wt% Sn, respectively).

A. Hrussanova (✉) · I. Krastev
“Rostislav Kaischew” Institute of Physical Chemistry,
Bulgarian Academy of Sciences, 1113 Sofia, Bulgaria
e-mail: antoanet@venera.ipc.bas.bg

G. Beck · A. Zielonka
Institute of Precious Metals and Metal Chemistry,
73525 Schwäbisch Gmünd, Germany

The aim of this paper is to study the properties of silver-tin alloys obtained from pyrophosphate-cyanide electrolytes containing salts of EDTA.

2 Experimental details

The composition of the investigated pyrophosphate-cyanide electrolyte is given in Table 1. The method of preparation of the electrolyte is described elsewhere [10].

The CV experiments were performed in a 50 cm³ three-electrode glass cell at room temperature without agitation of the electrolyte. The vertical working electrode (area 0.6 cm²) and the two counter electrodes were made of platinum. An Ag|AgCl reference electrode ($E_{\text{Ag|AgCl}} = -0.197$ V vs. SHE) was used. The reference electrode was placed in a separate cell filled with 3 M KCl solution (Merck), connected to the electrolyte cell by a Haber-Luggin capillary through an electrolyte bridge containing also 3 M KCl solution. All potentials are given against this reference electrode.

The experiments were carried out at room temperature by means of a computerized PAR 263A potentiostat/galvanostat using the Soft Corr II software.

The sweep rate was 25 mV s⁻¹.

Some of the coatings were deposited in a glass cell of 250 cm³ and other coatings intended for study of the internal stress (IS) were deposited in a cell of 400 cm³. Distilled water and pro analysi grade reagents were used. Silver anodes 2 × 1 or 10 × 3 cm (during IS measurements) were used. Coatings were deposited on 0.3 mm thick copper substrates of dimensions 2 × 1 or 7 × 1 cm (during IS measurements). The thickness of the coatings varied from 6 μm (on contact pins for measurement of contact resistance and plug-in forces) up to 40 μm (during IS measurements). Prior to deposition, the substrates were electrochemically degreased and pickled according to a standard procedure. In some cases, the substrates were

silver plated for several minutes in order to prevent contact deposition of silver when dipping into the electrolyte. All coatings are deposited at room temperature without agitation of the electrolyte.

The Ag and Sn percentage in the coatings depending on the electrolysis conditions was determined by X-ray fluorescence analysis (Fischerscope X-ray XDAL). The rate of deposition of the alloy (the thickness of the deposited coatings) was determined gravimetrically or on the basis of XRF measurements. Each point of the curves in Figs. 1 and 2 represents the average of at least nine measurements in three different heights of the electrodes. The surface morphology of the coatings was studied by optical and scanning electron microscopy (SEM). The phase analysis was performed by means of a Bruker D8 diffractometer or Philips PW 1050 diffractometer at 2θ angles from 28 to 82° with Cu_{Kα} irradiation and scintillation detector.

The internal stress, *IS*, was monitored with the apparatus constructed by Stalzer [11] and the method was described in a previous paper [12]. The method permits in situ *IS*-monitoring during electrodeposition. The density of the coating was calculated taking into account the composition of the alloy.

The microhardness, *H_v*, of the deposited (during IS measurements) coatings was measured with the apparatus Polyvar using a load of 3 p at different positions in the polished cross-section of the coatings. That ensures exact measurement and good reproducibility of the results.

The contact resistance, *R_Ω*, of 6 μm thick layers was measured by the Burster microohmmeter Resistomat 2323 on brass contact pins of diameter 4 mm and length 14 mm at a pressure force of 2 N. After the standard pre-treatment (electrochemical degreasing, rinsing and neutralisation), the pins were coated with Ag-Sn alloy in electrolyte 3. As reference samples, other pins were initially coated with nickel in Watts electrolyte containing 1 g dm⁻³ saccharin and 0.2 g dm⁻³ 2-Butin-1,4-diol (60 °C, 5 A dm⁻², 5 min)

Table 1 Composition of the electrolyte

Components	Composition/g dm ⁻³			
	Electrolyte 1	Electrolyte 2	Electrolyte 3	Electrolyte 4
Ag as KAg(CN) ₂	15.5	15.5	15.5	15.5
Sn as SnCl ₂ ·2H ₂ O	15.5	15.5	20.0	20.0
K ₄ P ₂ O ₇	137	137	137	137
KOH	8	8	8	–
Na ₂ EDTA·2H ₂ O	60	60	60	–
Na ₄ EDTA·2H ₂ O	–	–	–	60
H ₂ O ₂ (30%) (mL)	–	2	2	2
KCN	60	60	60	60
pH	9	9	9	11

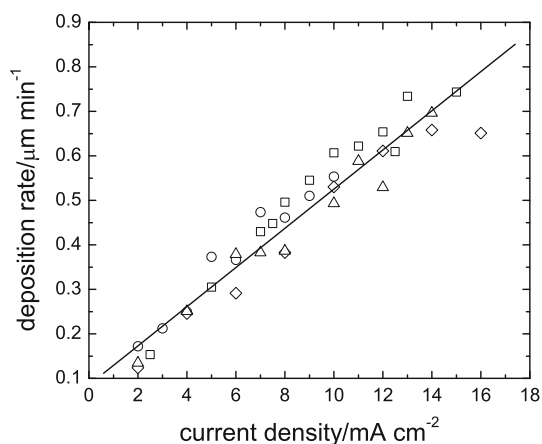


Fig. 1 Effect of the current density on the deposition rate of the Ag-Sn coatings: electrolyte 1 (square), electrolyte 2 (circle), electrolyte 3 (diamond), electrolyte 4 (triangle)

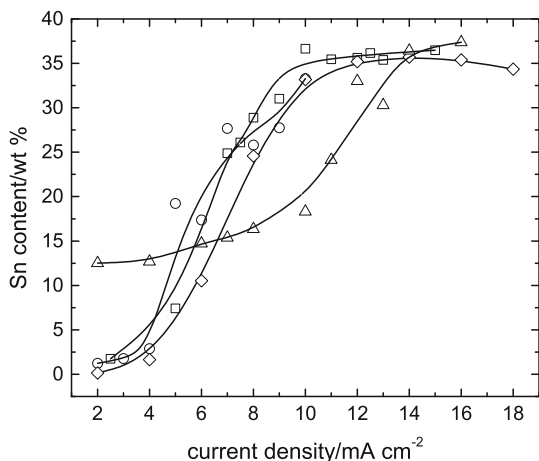


Fig. 2 Effect of the current density on the tin percentage in the coatings: electrolyte 1 (square), electrolyte 2 (circle), electrolyte 3 (diamond), electrolyte 4 (triangle)

and then with gold in the electrolyte Auruna 539 of Degussa (50 °C, 2.5 A dm⁻², 5 min).

The plug-in forces, F , were measured during the introduction of similar contact pins coated with a 6 μm thick deposit of Ag-Sn alloy into pure silver coated jacks using the apparatus Zwick/Roell Z 2.5. During the measurements, the pin was introduced into the jack at a constant velocity and the changes of the applied force with time were recorded.

After measurement of the internal stress, the abrasion resistance, A , of the same layers was determined according to the Bosch-Weinmann method. An abrasive disk (diameter 47 mm, width 10 mm) moves under constant load (3.92 N) back and forth on the tested surface. After each cycle, the disk rotates in a small step, so as to provide fresh abrasive surface. By appropriate choice of the grain size of the abrasive band, it is possible to control the intensity of

abrasion. In the present study, the latter was determined after 200 cycles using an abrasive band of grade 1000. The wear resistance was determined by the weight loss. It is defined as the number of cycles required for the erosion of 1 mm³ of the coating and is given by:

$$A = z(D/G)$$

where A is the wear resistance, D the density of the material (mg mm⁻³), z the number of cycles, G is the weight loss (mg).

3 Results and discussion

3.1 Deposition rate

The dependence of the deposition rate of the Ag-Sn coatings on the current density is almost linear and the differences corresponding to the different electrolytes are not essential (Fig. 1). The deposition rate varies between 0.2 and 0.7 μm per min depending on current density.

3.2 Alloy composition

The influence of the current density on the tin percentage in the coatings is shown in Fig. 2. The tin content in the coatings increases depending on the current density reaching a plateau at about 10 mA cm⁻² due to the deposition of the alloy at limiting current density (electrolytes 1–3). It is possible to obtain coatings from the investigated electrolytes with a tin content of up to about 38 wt%. This amount of tin is much higher than the saturation limit (12 wt% Sn in phase diagram [13] or 18 wt% in electrolytically obtained alloy [7]) of the silver lattice during the formation of solid solution of tin in silver. Possibly at higher tin content strong changes in the phase composition and in some properties of the obtained coatings could be observed.

The effect of pH due to the different type of the complexing agent on the tin content is stronger at low current densities. At pH 9 (in presence of Na₂EDTA) the tin content of the obtained coatings is lower than at pH 11 (in the presence of Na₄EDTA). Similar influence of pH on tin content in the coatings is observed by Kubota et al. [6]. They found that the tin content in the coating increased from 5 to 10 wt% with the increase in pH from 8–8.5 up to 9–9.5. Cyclic voltammetric measurements show the increased polarization during deposition in the presence of EDTA salts (Fig. 3, curves 1 and 2). In the presence of Na₂EDTA tin deposition is inhibited (lower cathodic peak) as compared to the case when Na₄EDTA is used. In the case of Na₂EDTA the dissolution of the deposited coating is more effective possibly due to stronger complex

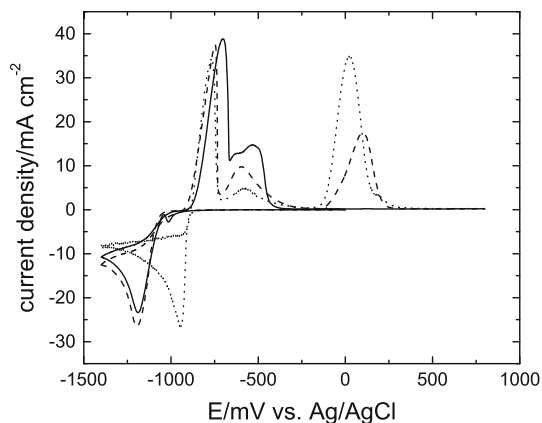


Fig. 3 Cyclic voltametric curves in different electrolytes: *solid line* $37.7 \text{ g dm}^{-3} \text{ SnCl}_2 \cdot 2\text{H}_2\text{O}$, $137 \text{ g dm}^{-3} \text{ K}_4\text{P}_2\text{O}_7$, $8 \text{ g dm}^{-3} \text{ KOH}$, $60 \text{ g dm}^{-3} \text{ Na}_2\text{EDTA}$ and $2 \text{ mL dm}^{-3} \text{ H}_2\text{O}_2$ (30%); *dashed line* $37.7 \text{ g dm}^{-3} \text{ SnCl}_2 \cdot 2\text{H}_2\text{O}$, $137 \text{ g dm}^{-3} \text{ K}_4\text{P}_2\text{O}_7$, $8 \text{ g dm}^{-3} \text{ KOH}$, $60 \text{ g dm}^{-3} \text{ Na}_4\text{EDTA}$ and $2 \text{ mL dm}^{-3} \text{ H}_2\text{O}_2$ (30%); *dotted line* $37.7 \text{ g dm}^{-3} \text{ SnCl}_2 \cdot 2\text{H}_2\text{O}$, $137 \text{ g dm}^{-3} \text{ K}_4\text{P}_2\text{O}_7$, $8 \text{ g dm}^{-3} \text{ KOH}$, and $2 \text{ mL dm}^{-3} \text{ H}_2\text{O}_2$ (30%); Sweep rate 25 mV s^{-1}

formation at the lower pH and the anodic maximum at about -100 mV is not registered. The observed anodic maxima show different anodic reactions connected with processes of passivation and formation of different tin complexes during dissolution.

3.3 Phase composition

Changes in the alloy composition can result in changes in the phase composition of the coatings. The silver is the more positive element in this electrochemical system and at low current densities deposits preferentially. In this case the reflexes in the X-ray diffractograms correspond to pure silver. At higher current densities the deposition potential of tin is reached and the co-deposited tin forms a solid solution with silver. According to the phase diagram of the alloy, the solid solution phase (α -phase) should be observed in the interval zero up to about 12 wt% of tin in metallurgical alloy (phase diagram) [13] or to about 18 wt% in electrolytically obtained alloy [7]. The increase of the tin content in this interval leads to some expansion of the silver lattice i.e., increase of the lattice parameter of silver, which results in an increase in the compressive internal stress of the deposit (see Fig. 5). XRD investigations show an increase of the lattice parameter of silver at tin contents of about 5 wt% (Fig. 4a, curve 1), as well as a preferred $\langle 111 \rangle$ -orientation of the crystallites of the alloy deposit. This orientation is typical for silver coatings deposited from electrolytes containing silver cyanide complexes [14]. The width of the reflexes confirms the presence of a fine crystalline coating. At twice higher tin content (about 10 wt%) in the deposit, the shift of the reflexes towards lower 2θ -angles confirm the further expanding of the silver

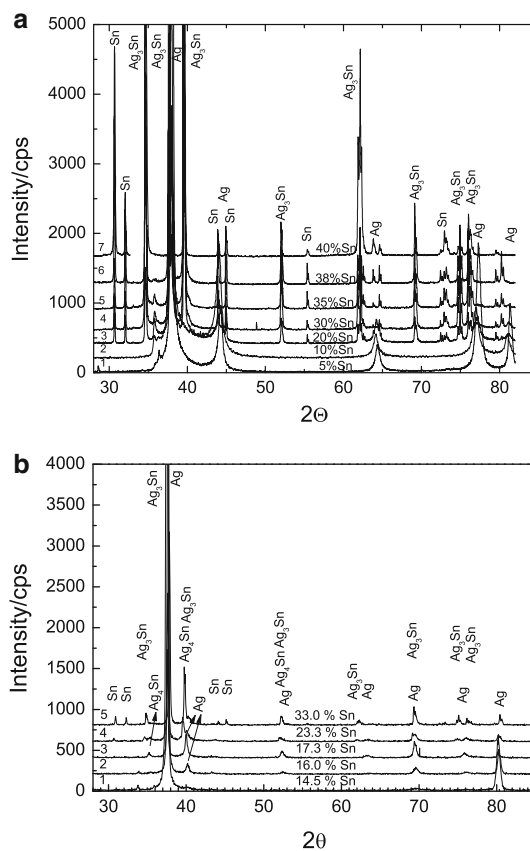


Fig. 4 **a** X-ray diffractograms of Ag-Sn alloy coatings with different tin content, obtained in electrolyte 3. **b** X-ray diffractograms of Ag-Sn alloy coatings with different tin content, obtained in electrolyte 4

lattice together with the decrease in the grade of the $\langle 111 \rangle$ -orientation. Up to 16 wt% only α -phase is present in the corresponding diffractograms (Fig. 4a, b). This is in good agreement with the data obtained by Grekova and Vyacheslavov [7]. The silver lattice should be saturated with tin atoms at about 18 wt% Sn and the deposition of higher tin amounts results in the deposition of a new tin-rich phase. At about 17.3 wt% tin new phase is observed— Ag_4Sn (Fig. 4b curve 3). This is in good agreement with the data obtained by Grekova and Vyacheslavov [7]. Mixture of pure tin-phase and ϵ -phase (Ag_3Sn) is found at tin content from 25 to 100 wt% in metallurgical alloy [13], while in the electrolytically obtained alloy pure tin phase could be detected even at lower tin content—19 wt%. The X-ray spectra of the coatings obtained in electrolytes 3 and 4 are in agreement with these data.

The analysis of the respective diffractogram (Fig. 4a, b curves 3, 4, respectively) shows the presence of the pure tetragonal tin phase and the orthorhombic mixed phase Ag_3Sn . Small reflexes near to the theoretical positions of the reflexes of the Ag_4Sn -phase are observed in this case. Possibly, they belong to this phase, but with an increased lattice parameter. The registered phases are not oriented

and the size of the crystallites is obviously bigger (curve 3). The amount of the α -phase decreases markedly at higher tin contents in the coating (Fig. 4a). At tin contents of about 30 wt% the registered phases are not oriented, but at higher tin contents the tin-richer phases become oriented (textured) and at about 35 wt% Sn the Ag_3Sn -phase shows an $\langle 201 \rangle$ -orientation (curve 5).

At 38 wt% Sn in the coatings the pure tin phase has a mixed texture along the axes $\langle 200 \rangle$ and $\langle 220 \rangle$ and the texture of the Ag_3Sn -phase changes in $\langle 020 \rangle$.

The tin phase is oriented along the $\langle 200 \rangle$ axis and the $\langle 201 \rangle$ -, $\langle 203 \rangle$ - and $\langle 400 \rangle$ -reflexes of the orthorhombic Ag_3Sn -phase grow with the increased tin content. In this case the volume of the Ag_3Sn -phase predominates over the other phases of the alloy.

The XRD-investigations allow the conclusion, that the silver-rich phase is the only phase observed up to 16 wt% Sn in the alloy coating. At higher tin contents additionally Ag_3Sn , Ag_4Sn and a pure tin phase are observed. The coatings are textured, changes in the preferred orientation of the crystallites in the deposit can be observed. The changes in the elemental and in the phase composition respectively should result in the respective changes in the properties of the deposits.

3.4 Internal stress

The changes in the internal stress, IS , during electrodeposition are illustrated in Fig. 5 for different current densities.

Low positive (tensile) stress is observed in the silver coatings electrodeposited from cyanide electrolytes [11, 14, 15]. Tin coatings show negative (compressive) internal stress [17]. Low stress values of about -0.6 N mm^{-2} were measured. The X-ray investigations of the alloy coatings show the expansion of the silver lattice due to the formation of solid solution of tin in silver (α -phase), which

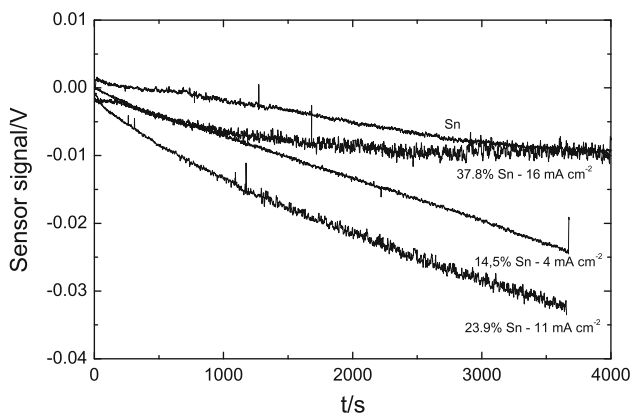


Fig. 5 Sensor signal during IS measurements in Sn and Ag-Sn alloy deposition from electrolyte 4

results in the appearance of negative (compressive) internal stress in the electrodeposited alloy coatings (Fig. 5, curve 14.5 wt% tin; -9.8 N mm^{-2}). At higher tin contents (23.9 wt%) negative internal stress is still observed (-4.7 N mm^{-2}), in spite of the higher total tin amount in the alloy than the saturation limit of the silver lattice (about 18 wt%). The increased tin content leads to the formation of heterogeneous coatings consisting of different alloy phases, each of them contributing to the measured internal stress. In this case the XRD-investigations show also the presence of the Ag_3Sn -phase. At very high tin amount almost stress free incompact coatings are deposited.

3.5 Microhardness

Microhardness, H_v , is a structure sensitive property of every alloy and depends on its composition. It was established that the co-deposition of tin leads to an increase in H_v up to 18 wt% Sn (Fig. 6). At a higher tin content H_v significantly decreases due to deposition of heterogeneous multiphase coatings at higher current densities. Similar dependence of the microhardness on tin content is observed and Grekova and Vycheslavov [7]. The latter showed that maxima in the curves for microhardness, specific electrical resistivity and contact resistance are observed at tin contents corresponding to the α -, ζ - and ε -phases (5, 15 and 28 wt%, respectively). Nutsch et al. [8] present results for microhardness of Ag-Sn coating in wide range of Sn contents in the alloys—from 8.9 to 42 wt% and observed the highest value for microhardness for the alloy containing around 20 wt% tin, which is in agreement with our results. Leidheiser and Ghuman [8] measured the microhardness of Ag-Sn coatings with tin content from 18 to 40 wt%. In this region the microhardness decreases with the increase in tin content (the existence of a small maximum at about 25–27 wt% Sn could be supposed in the reported curve). Further decrease in the microhardness is reported by

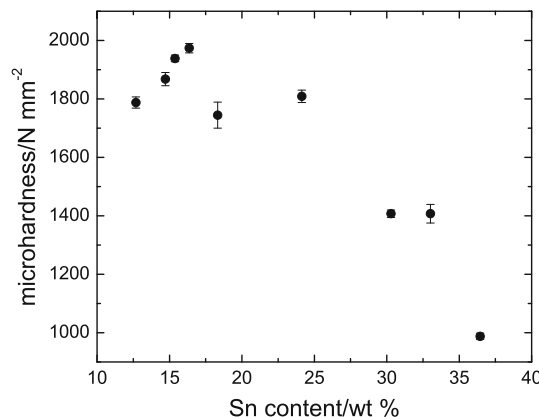


Fig. 6 Effect of the tin content on the microhardness (H_v) of the alloys from electrolyte 4

Kubota and Sato [6] at very high tin contents in the alloy deposits.

3.6 Contact resistance

The contact resistance, R_{Ω} , of the Ag-Sn coatings increases at higher current densities, i.e., at a higher Sn content in the deposit (Fig. 7). Linear dependencies of R_{Ω} versus i ($0.2 \mu\Omega$ per 10 mA cm^{-2}) were established by measurements of the alloy coatings against a gold-plated substrate or alloy samples of the same composition. The contact resistance depends non-linearly on tin content in the investigated current range, may be due to the observed phase heterogeneity in the coatings. Strong increase in R_{Ω} at lower tin content and smaller changes at higher tin content are observed. The differences between the values obtained against gold or silver-tin alloy coatings are not essential.

3.7 Plug-in forces

The force, F , measured upon introduction of the pin into the jack grows proportionally to the contact area and reaches its maximum when the pin is fully inserted into the jack. Taking into account the dependence of F on the contact area, i.e., bearing in mind that the maximum value of the contact force would be different for pins and jacks with the same properties of the coating, but of different size, the slope of the time dependence of F could also be proposed as a measure of the friction properties (plug-in forces) of the coatings obtained. The slope of the time dependence of the plug-in force F on the current density is shown on Fig. 8. Similar to the plug-in forces of some other silver alloys such as Ag-Sb [12], Ag-In [15] and Ag-Bi [16] the slope decreases with the rise in current

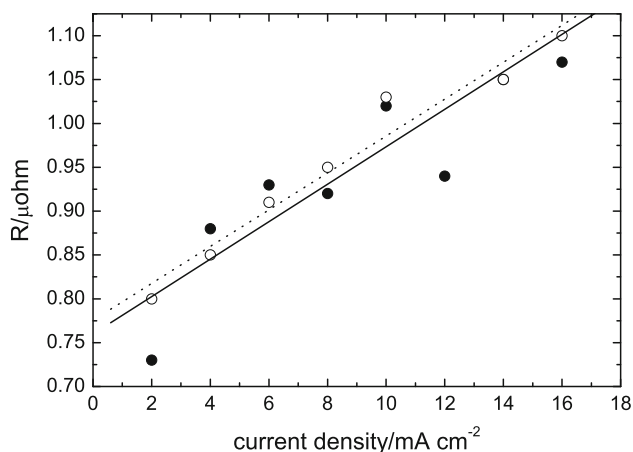


Fig. 7 Effect of the current density (tin content) on contact resistance (R_{Ω}) measured against (filled circle) gold and (open circle) the same alloy from electrolyte 3

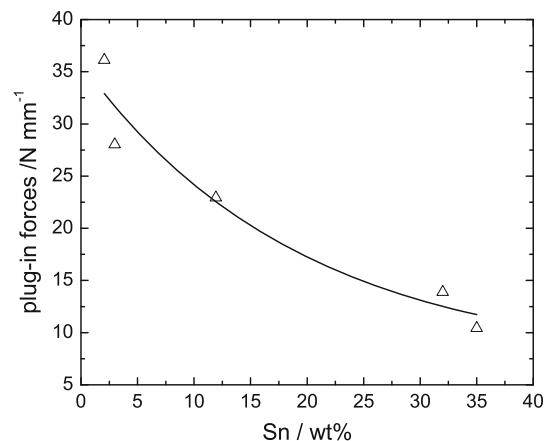


Fig. 8 Effect of the tin content in Ag-Sn alloys from electrolyte 3 on the plug-in forces (F) measured against silver-plated jacks

density, i.e., by increased Sn content in the alloy that shows the lubricating properties of the alloy as compared to pure silver.

3.8 Abrasion resistance

Almost linear reduction in the abrasion resistance is obtained with the increase in current density, i.e., in Sn content in the coating (Fig. 9). Similar dependencies are obtained for Ag-Sb [12] and Ag-In [15] alloys. The abrasion resistance of the coatings is higher than this of Ag-In and lower than that of Ag-Sb alloys.

By co-deposition of Sn, semi bright coatings can be obtained. Under certain conditions, the different phases can self-organize on the coating surface in ordered structures, as shown in Figs. 10 and 11. Figure 10 presents an alloy coating on an electrical contact pin. The phase heterogeneity of the alloy is well visible and the tin reach dark

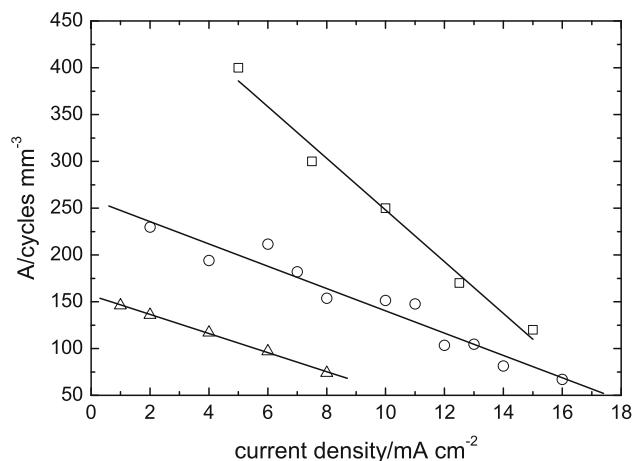


Fig. 9 Effect of current density on the abrasion resistance of Ag-Sn from electrolyte 4 (circle), Ag-Sb (square) and Ag-In (triangle) alloy coatings



Fig. 10 Surface of an Ag-Sn alloy coating deposited from electrolyte 3 on a contact pin at 14 mA dm^{-2}

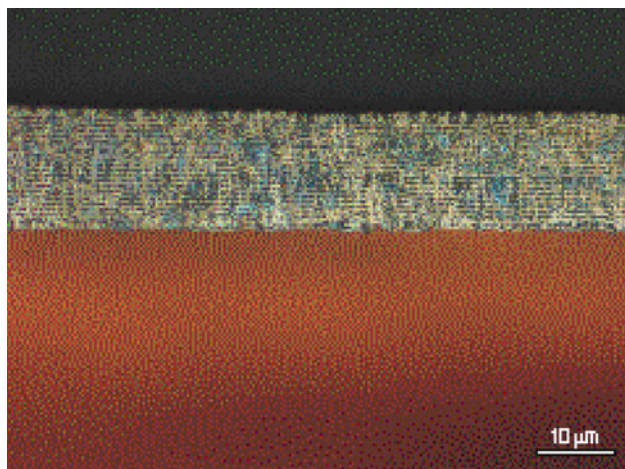


Fig. 11 Cross-section of an Ag-Sn alloy coating obtained from electrolyte 4 at 12 mA dm^{-2}

stripes are moving upwards over the surface during deposition.

At certain conditions this movement could result in the formation of layered structure without applying external

electrical pulses during deposition. The cross-section of a similar coating on a flat copper substrate is shown in Fig. 11. The strong periodicity of the self-structured coating is impressive.

4 Conclusions

The co-deposition of tin leads to the change of the tensile stress of pure silver coatings to compressive stress of the formed solid solution of the alloy and to almost stress free coatings at high current densities. The microhardness runs over a maximum at current densities, where the silver lattice is saturated with tin and phase heterogeneous coatings are deposited. The abrasion resistance diminishes at increased tin content, and the changes of the electrical contact resistance are in the opposite direction. The measured plug-in forces show the lubricating properties of the alloy coatings.

Acknowledgments The authors are thankful to Deutsche Forschungsgemeinschaft (DFG) for the support of Project 436 BUL 113/97-0-4. The authors are thankful to National Science Fond for the support of Project BG051P0001/07/33-02/40.

References

1. John WG, Evans EI (1937) *Phil Mag* 23:1033
2. Dornblatt AJ (1940) In: Addicks L (ed) *Silver in the industry*. Reinhold Publishing Corporation, New York
3. Buckner Speed J, Falk AH (1925) US Patent 1,565,115
4. Leach RH (1934) US Patent 1,952,082
5. Puipe JC, Fluehmann W (1983) *Plat Surf Finish* 70:46
6. Kubota N, Sato E (1985) *Electrochim Acta* 30(3):305
7. Grekova NA, Vyacheslavov PM (1971) *Zh Prikl Khim* 44:1975
8. Leidheiser H Jr, Ghuman ARP (1973) *J Electrochem Soc* 120:484
9. Nutsch R, Liebscher H, Degner W et al (1993) *Galvanotechnik* 84:425
10. Hrussanova A, Krastev I (2009) *J Appl Electrochem* 39(7):989
11. Stalzer M (1964) *Metalloberfläche* 18:263
12. Krastev I, Petkova N, Zielonka A (2002) *J Appl Electrochem* 32:811
13. Hansen M, Anderko K (1962) *Strukturi dwojnih splawow*, Metallurgizdat, Moscow (in Russian)
14. Kristev I, Nikolova M (1986) *J Appl Electrochem* 16:867
15. Krastev I, Dobrovolska Ts, Kowalik R, Zabinski P, Zielonka A (2009) *Electrochim Acta* 54:2515
16. Krastev I, Valkova T, Zielonka A (2004) *J Appl Electrochem* 34:79
17. Tushinsky L, Kovensky I, Plokhov A, Sindeev V, Reshedko P (2002) *Coated metal, structure and properties of metal coatings composition*. Springer-Verlag, Berlin